Int. J. Solids Structures Vol. 28, No. 3, pp. 283–297, 1991
Printed in Great Britain.

0020-7683/91 $3.00 + .00

ANALYSIS OF A BROKEN FIBER IN A WEAKLY BONDED COMPOSITE

H. R. SCHWIETERT and P. S. STEIF
Department of Mechanical Engineering, Carnegie Mellon University, Pittsburgh, PA 15213-3890, U.S.A.

(*Received* 2 *April* 1990; *in revised form* 10 *September* 1990)

Abstract—The problem of a broken fiber, embedded in an infinite medium with distinct elastic properties, is studied theoretically. The composite is subjected to tensile loading parallel to the fiber. To simulate the influence of a weak fiber–matrix interface, interfacial slippage governed by a Coulomb friction law is permitted. The solution method that is employed reduces the problem to four coupled singular integral equations which are solved numerically. Results for the average axial fiber stress, for the enhancement in the tensile stress in the matrix and for the opening of the crack are presented; where relevant, comparisons are made with simplified, highly approximate methods of analysis.

1. INTRODUCTION

Failure in fiber-reinforced composites is generally preceded by the development of damage. Among the most common forms of damage are fiber breaks and matrix cracks. In ceramic–matrix composites, matrix cracks appear at lower stresses due to the lower ductility of the matrix, while fibers begin to fail at stresses approaching the ultimate strength. The study of the stress redistribution associated with the development of damage is of interest for several reasons: for example, damage alters the subsequent stress–strain behavior, and damage eventually coalesces in some way to cause failure. This paper is concerned, in particular, with the redistribution of the stresses associated with the breaking of a fiber.

The first serious attempt at a solution to the problem of a broken fiber appears to be that of Muki and Sternberg (1971), who treated the fiber as a one-dimensional continuum, from which it was possible to develop an integral equation for the force carried by the fiber. A rigorous, fully three-dimensional solution to this problem was developed by Ford (1973), who considered both the load transfer back to the broken fiber, which was of interest to Muki and Sternberg, as well as the stress intensity factors.

In so far as its relevance to many real composites, however, the problem studied by Muki and Sternberg (1971) and Ford (1973) is deficient in one important respect: it presumes perfect bonding at the fiber–matrix interface. By contrast, the interfaces of many composites are far from perfect; indeed, the strength—or weakness—of the interface is consistently cited as having a major influence on composite properties. Since the effects of damage, particularly fiber breaks, are highly sensitive to interface conditions, methods of analyzing damage in the presence of an imperfect interface are potentially of great value. Herein, we present a rather general, highly accurate method for analyzing the stress redistribution associated with a broken fiber; besides its applicability to the case of perfect bonding at the interface, this method, as will be seen, can handle a wide variety of interface laws.

We illustrate this method of analysis and its predictions by employing a simple interface model which may be relevant to ceramic–matrix composites. In some brittle–matrix composites there appears to be no chemical bonding at the interface; instead, the fiber and matrix are coupled by friction or mechanical interlocking (Phillips, 1974; Prewo and Brennan, 1980). These experimental observations have suggested the plausibility of a frictional model for the interface. Using a Coulomb friction law for the interface, Dollar and Steif (1989) considered the two-dimensional broken fiber problem, under the assumption that the elastic moduli of the fiber and matrix are identical. They found the stresses near the fiber break to be *nonsingular*, with the *stress concentration* dependent on the interface

parameters and on the applied load. Furthermore, the rate at which load is transferred back to the fiber is significantly slower than the transfer rate assuming perfect bonding, more consistent with simplified shear-lag style analyses. Wang *et al.* (1989) showed that the method of Dollar and Steif (1989) involving distributed dislocations may be generalized to cases where the fiber and matrix have different moduli, provided the slip length is vanishingly small compared with the break.

With the eventual goal of treating the full three-dimensional bimaterial broken fiber problem with a frictional interface, the present authors recently developed an interface integral equation method. As a test of this method, we applied it to the two-dimensional bimaterial broken fiber problem (Schwietert and Steif, 1991); by comparison with known solutions, this method was shown to provide rather accurate numerical solutions. In the present paper, we demonstrate that this method is readily modified to handle axisymmetric three-dimensional problems, in particular the broken fiber problem that is of concern here. As has been appreciated by others, the rate of load transfer to the broken fiber is of central importance to the residual strength and the subsequent stiffness of the damaged composite. Hence, a principal focus here will be on the nature of the load transfer and its dependence on interface and material parameters. In addition, we will present results for the stress enhancement near the break, as well as for the crack-tip opening displacement.

2. PROBLEM DESCRIPTION

The problem we are considering is shown schematically in Fig. 1 and is best described with a polar coordinate system (r, θ, z). An infinitely long fiber of circular cross-section, occupying $0 < r < a$, $0 < \theta \leqslant 2\pi$, is embedded inside an infinite medium, the matrix. The fiber and the matrix are homogeneous, isotropic and linear elastic, with shear modulus and Poisson ratio G_1, ν_1 and G_2, ν_2, respectively. A residual state of stress is assumed to exist, in which the normal stress at the interface is compressive ($\sigma_{rr} = -\sigma_0 < 0$) and there is no

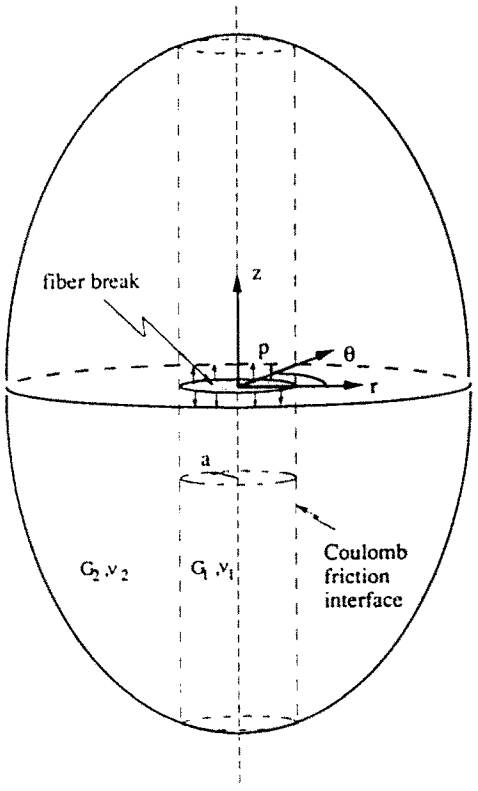

Fig. 1. Schematic of a cracked fiber in infinite medium, which is opened with a pressure p.

residual shear stress at the interface; the fiber–matrix interface is capable of slip according to a Coulomb friction law. The fiber is broken at $z = 0$ over its entire cross-section, resulting in a penny-shaped crack of radius a. The crack faces are subjected to an opening pressure p.

A point-wise Coulomb friction law is employed here to model the interfaces. According to this friction law, at any instant in the loading history either sticking, slipping or opening occurs at a generic point along the interface. Conditions for these three states along the interface $r = a$ are as follows:

$$\text{stick condition} \quad \sigma < 0, |\tau| < \mu|\sigma|, \frac{dg}{dt} = 0, h = \frac{dh}{dt} = 0 \tag{1a}$$

$$\text{slip condition} \quad \sigma < 0, |\tau| = \mu|\sigma|, \operatorname{sgn}\left(\frac{dg}{dt}\right) = \operatorname{sgn}(\tau), h = \frac{dh}{dt} = 0 \tag{1b}$$

$$\text{open condition} \quad \sigma = \tau = 0, h > 0 \tag{1c}$$

with

$$\sigma = \sigma_{rr} \quad \tau = \sigma_{rz} \tag{2a,b}$$

$$g = \lim_{\varepsilon \to 0^+} [u_z(a+\varepsilon, z) - u_z(a-\varepsilon, z)] \tag{2c}$$

$$h = \lim_{\varepsilon \to 0^+} [u_r(a+\varepsilon, z) - u_r(a-\varepsilon, z)]. \tag{2d}$$

In these equations u_r and u_z denote the r- and z-components of displacement, respectively, μ is the friction coefficient which is assumed to be constant along the interface, and $d(\ )/dt$ denotes the derivative with respect to a time-like parameter that increases monotonically as the loading proceeds. The condition $\operatorname{sgn}(dg/dt) = \operatorname{sgn}(\tau)$ is the condition of positive energy dissipation which dictates that the instantaneous increment of slip be in the same direction as the shear stress. Note that we ignore the distinction between static and kinetic friction.

We wish to point out the connection between the problem just posed and the problem of a broken fiber under a *remote* load. In general, the composite will have residual stresses which arise during its fabrication and processing. This distribution of residual stresses will be quite complicated (practically defying analysis), but is likely to be described rather crudely as follows. There is a residual longitudinal normal stress σ_F in the fiber and σ_M in the matrix (one tensile, one compressive), and there is a residual radial tension or compression σ_n at the interface. These stresses are often estimated with a concentric cylinder analysis which uses the Lamé solution [see, for example, Timoshenko and Goodier (1970)]. Let there also be a remotely applied longitudinal tension. By itself, this remote tension causes the stress in the fibers to be σ_∞ and, in general, gives rise to a radial stress σ_{rad} at the interface. (σ_{rad} is uniform to the same degree of approximation as the residual stress σ_n is uniform.)

Consider now the problem of a single broken fiber in an infinite medium which has the stresses just described; the broken fiber must have zero tractions across the crack faces. Of particular interest is the feasibility of decomposing this problem into one involving pressure applied to the crack faces. If one were analyzing a composite with a *perfectly bonded interface*, then one would only need to solve the problem of opening the crack faces with a pressure which is equal to $\sigma_\infty + \sigma_F$ (while the remote stresses are zero); the piecewise constant stresses associated with the remote stress and all the residual stresses can then be simply added back in the end. In the case of a Coulomb friction interface, however, it is necessary to account for the total tractions at the interface. This can be done by again considering the opening of the crack faces with a pressure $\sigma_\infty + \sigma_F$. The shear stress σ_{rz} at the interface associated with this pressurization loading is the only shear stress in the problem. The total normal stress at the interface, however, includes contributions from the residual stresses, from the remote load, as well as from the pressurization loading. Thus,

to solve the problem with the pressurization loading, one must include an effective residual normal stress $\sigma_{rr} = -\sigma_0 = \sigma_n + \sigma_{rad}$, where it is assumed that $\sigma_n + \sigma_{rad} < 0$. Note that σ_0 actually changes with the load through the term σ_{rad}, although here we do not account explicitly for any variation of σ_0 with σ_z. The longitudinal stresses can again be added back at the end without changing the essential features of the solution associated with the crack or the interface.

In analyzing this problem, it is of interest to examine the nature of the stress field near the perimeter of the penny-shaped crack. Experience with other problems involving cracks impinging on frictional interfaces (Dollar and Steif, 1989; Schwietert and Steif, 1991) suggests that the stresses in the vicinity of the fiber break are, in fact, nonsingular. To see that this carries over to the three-dimensional axisymmetric problem, we appeal to Zak (1964), who showed that the stress *singularities* at cylindrical corners in axisymmetric problems correspond to those of plane strain problems with equivalent boundary conditions. This equivalence can be appreciated by noting that the hoop strain must be bounded as it is given by $\varepsilon_{\theta\theta} = u_r/r$; thus, it is negligible in comparison with the radial and axial strains which are singular. Therefore, to demonstrate the *absence* of singular stresses in the three-dimensional problem, it is sufficient to show the absence of singular stresses in the analogous two-dimensional plane strain problem. Once this is demonstrated, however, one can expect the forms of the *finite* near-tip stress fields to be different in the two cases: the axisymmetric strain state is not effectively plane strain now, since the hoop strain is no longer negligible in comparison with the other strains.

It is, therefore, sufficient to consider the configuration of Fig. 2 and search for separable stress fields of the form $\sigma \sim \rho^{\lambda-1}$, where ρ is the distance from the crack tip and admissible values of λ are in the range $0 < \mathrm{Re}(\lambda) < 1$. In Schwietert and Steif (1991) the possibility of singular stress fields for this configuration was analyzed, for different values of the Dundurs (1967) bimaterial parameters

$$\alpha = \frac{G_2(\kappa_1+1) - G_1(\kappa_2+1)}{G_2(\kappa_1+1) + G_1(\kappa_2+1)} \qquad \beta = \frac{G_2(\kappa_1-1) - G_1(\kappa_2-1)}{G_2(\kappa_1+1) + G_1(\kappa_2+1)}$$

where $\kappa_1 = 3-4\nu_1$ and $\kappa_2 = 3-4\nu_2$ in plane strain.

It was found that for most relevant values of α, β and μ, there are no admissible stress singularities. For example if $\mu = 0.3$, singularities are only possible for extreme moduli ratios ($G_1/G_2 \approx 50$). This remains essentially true for large values of μ as well. As mentioned in the Introduction, our concern is mainly with fiber-reinforced ceramics; the moduli of the constituents of these materials are typically not so different. Hence, it can be concluded that no stress singularities will be present for *relevant* combinations of moduli. For other composite systems, such as graphite fibers in an epoxy matrix, mild singularities are possible.

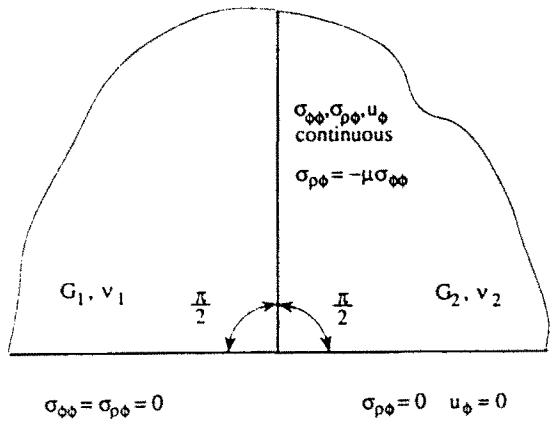

Fig. 2. Configuration and boundary conditions for the near-tip stress analysis.

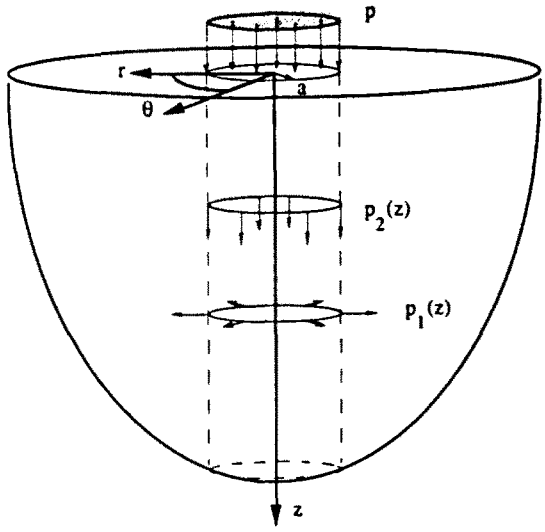

Fig. 3. Schematic of body 1, a homogeneous half-space of fiber material, G_1, ν_1.

3. METHOD OF SOLUTION

In this section we will present the integral equation method which is used to solve the problem considered here. This method was developed earlier (Schwietert and Steif, 1991) for solving two-dimensional problems and is extended here to three-dimensional axisymmetric problems. We will take advantage of the symmetry about the plane $z = 0$ and solve the problem for the upper half of the composite ($z > 0$). The method requires the introduction of two auxiliary bodies.† Consider body 1 which is a homogeneous half-space having the same moduli as the fiber. In the portion $0 < r < a$, $0 < \theta \leqslant 2\pi$ and $0 < z < \infty$ of body 1, we will set up the same stress and displacement fields as exist in the corresponding portion of the composite body. To do this, we apply a uniform pressure p over $0 < r < a$, $0 < \theta < 2\pi$, $z = 0$ and zero tractions over the rest of the surface $z = 0$. In addition, we apply a distribution of ring forces $\mathrm{d}\mathbf{f} = \mathrm{d}f_r\mathbf{e}_r + \mathrm{d}f_z\mathbf{e}_z$ (see Fig. 3)

$$\mathrm{d}f_r\mathbf{e}_r + \mathrm{d}f_z\mathbf{e}_z = p_1(z)\mathbf{e}_r\,\mathrm{d}z + p_2(z)\mathbf{e}_z\,\mathrm{d}z \quad \text{on } r = a,\ 0 < \theta \leqslant 2\pi,\ 0 < z < \infty. \tag{3}$$

Note that these body forces, which preserve axisymmetry about the z-axis, must be applied so as to induce no additional tractions on the plane $z = 0$. Of particular interest will be the tractions and displacement gradients at $r \to a^-$, where a^- is defined as

$$a^- \equiv \lim_{\substack{\varepsilon \to 0 \\ \varepsilon > 0}} (a - \varepsilon).$$

We denote these tractions and displacement gradients by σ^F_{rr}, σ^F_{rz}, $u^F_{r,z}$ and $u^F_{z,z}$. By suitably adjusting the distributions $p_1(z)$ and $p_2(z)$, one can produce any distribution of tractions at the surface $r = a^-$. (Note that the stresses and displacement gradients can be discontinuous across the surface of body forces; however, we are only interested in field quantities inside $0 < r < a$.) The goal is to produce the correct σ^F_{rr}, σ^F_{rz}, $u^F_{r,z}$ and $u^F_{z,z}$; namely, those values of stress and displacement gradients along $r = a^-$ that equal the corresponding values in the composite body. Then, since the stress and displacement fields inside $0 < r < a$ depend uniquely on σ^F_{rr}, σ^F_{rz}, $u^F_{r,z}$ and $u^F_{z,z}$ (and on p), the same stress and displacement fields will exist inside $0 < r < a$ of body 1 as in the corresponding portion of the composite body.

† Our method is in some ways similar to that employed by Ford (1973), who also introduces auxiliary bodies. His method, in which a penny crack solution is built in, has the advantage that the homogeneous, perfectly bonded solution emerges exactly, while it does not in our method. On the other hand, our method is more convenient to apply to problems in which the stress is nowhere singular.

Consider now body 2 which is a homogeneous, infinite body having the same moduli as the matrix. In the portion $r > a$ of body 2 we will set up the same stress and displacement fields as exist in the corresponding portion of the composite body. To do this, we apply a distribution of ring forces $\mathrm{d}\mathbf{f} = \mathrm{d}f_r\mathbf{e}_r + \mathrm{d}f_z\mathbf{e}_z$ (see Fig. 4)

$$\mathrm{d}f_r\mathbf{e}_r + \mathrm{d}f_z\mathbf{e}_z = p_3(z)\mathbf{e}_r\,\mathrm{d}z + p_4(z)\mathbf{e}_z\,\mathrm{d}z \quad \text{on } r = a, 0 < \theta \leqslant 2\pi, -\infty < z < \infty \tag{4}$$

where $p_3(z) = p_3(-z)$ and $-p_4(z) = p_4(-z)$.

Note that these body forces preserve symmetry about the plane $z = 0$, as well as axisymmetry. Now the tractions and displacement gradients at $r \to a^+$ will be of particular interest. Here, a^+ is defined as

$$a^+ \equiv \lim_{\substack{\varepsilon \to 0 \\ \varepsilon > 0}} (a+\varepsilon). \tag{5}$$

We denote these tractions and displacement gradients by σ_{rr}^{M}, σ_{rz}^{M}, $u_{r,z}^{\mathrm{M}}$ and $u_{z,z}^{\mathrm{M}}$. By suitably adjusting the distributions $p_3(z)$ and $p_4(z)$, one can produce any distribution of tractions and displacements at the surface $r = a^+$. (Discontinuities again exist across the surface of body forces; however, now we are only interested in field quantities in the region $r > a$.) The goal is to produce the correct σ_{rr}^{M}, σ_{rz}^{M}, $u_{r,z}^{\mathrm{M}}$ and $u_{z,z}^{\mathrm{M}}$; namely, those values of stress and displacement gradients along $r = a^+$ that equal the corresponding values in the composite body. Then, since the stress and displacement fields in the region $r > a$ depend uniquely on σ_{rr}^{M}, σ_{rz}^{M}, $u_{r,z}^{\mathrm{M}}$ and $u_{z,z}^{\mathrm{M}}$, the same stress and displacement fields will exist inside these regions as in the corresponding portion of the composite body.

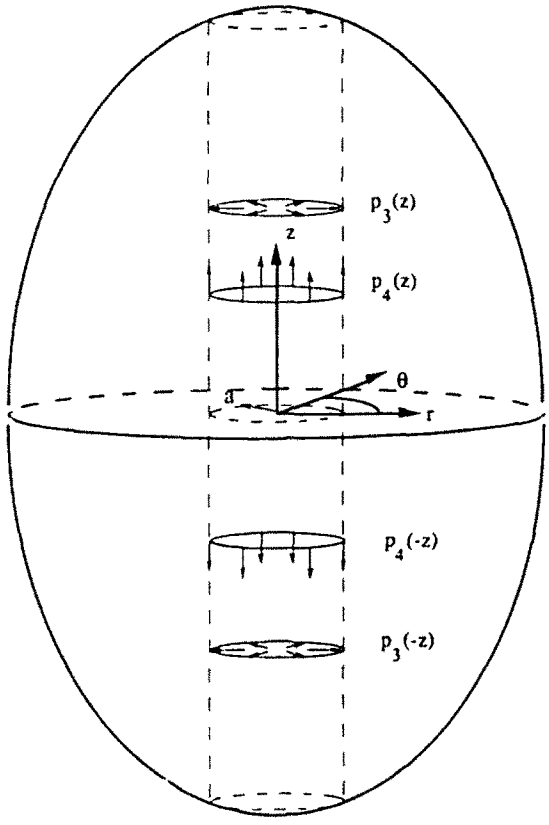

Fig. 4. Schematic of body 2, a homogeneous infinite body of matrix material, G_2, ν_2.

The nature of the interface in the composite material will determine the appropriate relationship between σ_{rr}^{F}, σ_{rz}^{F}, u_{rz}^{F}, u_{zz}^{F} and σ_{rr}^{M}, σ_{rz}^{M}, u_{rz}^{M}, u_{zz}^{M}. In the case that the conditions for a Coulomb friction interface prevail, this relationship is given by:

$$\sigma_{rr}^{F} = \sigma_{rr}^{M}, \sigma_{rz}^{F} = \sigma_{rz}^{M}, u_{rz}^{F} = u_{rz}^{M}, u_{zz}^{F} = u_{zz}^{M} \quad \text{stick zone.} \tag{6a}$$

$$\sigma_{rr}^{F} = \sigma_{rr}^{M}, \sigma_{rz}^{F} = \sigma_{rz}^{M}, u_{rz}^{F} = u_{rz}^{M}, \sigma_{rz} = -\mu\sigma_{rr} \quad \text{slip zone.} \tag{6b}$$

$$\sigma_{rr}^{F} = \sigma_{rr}^{M} = 0, \sigma_{rz}^{F} = \sigma_{rz}^{M} = 0 \quad \text{open zone.} \tag{6c}$$

The functions $p_1(z)$, $p_2(z)$, $p_3(z)$ and $p_4(z)$ have to be adjusted in such a way that eqns (6) hold along appropriate portions of $0 < z < \infty$. Then, the region $0 < r < a$ of body 1 can be matched up with region $r > a$ of body 2, yielding the solution to the problem.

Expressions for σ_{rr}^{F}, σ_{rz}^{F}, u_{rz}^{F} and u_{zz}^{F} in terms of p, $p_1(z)$ and $p_2(z)$ and σ_{rr}^{M}, σ_{rz}^{M}, u_{rz}^{M} and u_{zz}^{M} in terms of $p_3(z)$ and $p_4(z)$ are given by the following:

$$\sigma_{rr}^{F} = pA_0(z) + \tfrac{1}{2}p_1(z) + \int_0^{\infty} p_1(z')A_1(z,z')\,dz' + \int_0^{\infty} p_2(z')A_2(z,z')\,dz' \tag{7a}$$

$$\sigma_{rz}^{F} = pB_0(z) + \tfrac{1}{2}p_2(z) + \int_0^{\infty} p_1(z')B_1(z,z')\,dz' + \int_0^{\infty} p_2(z')B_2(z,z')\,dz' \tag{7b}$$

$$u_{rz}^{F} = pC_0(z) + \int_0^{\infty} p_1(z')C_1(z,z')\,dz' + \int_0^{\infty} p_2(z')C_2(z,z')\,dz' \tag{7c}$$

$$u_{zz}^{F} = pD_0(z) + \int_0^{\infty} p_1(z')D_1(z,z')\,dz' + \int_0^{\infty} p_2(z')D_2(z,z')\,dz' \tag{7d}$$

$$\sigma_{rr}^{M} = -\tfrac{1}{2}p_3(z) + \int_0^{\infty} p_3(z')A_3(z,z')\,dz' + \int_0^{\infty} p_4(z')A_4(z,z')\,dz' \tag{8a}$$

$$\sigma_{rz}^{M} = -\tfrac{1}{2}p_4(z) + \int_0^{\infty} p_3(z')B_3(z,z')\,dz' + \int_0^{\infty} p_4(z')B_4(z,z')\,dz' \tag{8b}$$

$$u_{rz}^{M} = \int_0^{\infty} p_3(z')C_3(z,z')\,dz' + \int_0^{\infty} p_4(z')C_4(z,z')\,dz' \tag{8c}$$

$$u_{zz}^{M} = \int_0^{\infty} p_3(z')D_3(z,z')\,dz' + \int_0^{\infty} p_4(z')D_4(z,z')\,dz' \tag{8d}$$

where the kernels $A_i(z,z')$, $B_i(z,z')$, $C_i(z,z')$ and $D_i(z,z')$ are derived from the solutions for a ring load in a half-space ($i = 1,2$) and from the solutions for a ring load in an infinite space ($i = 3,4$). These ring load solutions can be found by applying the Hankel transform to the governing equation and boundary conditions (Sneddon, 1951), and are given in the Appendix. With the results of Eason *et al.* (1955), the resulting integrals can then be expressed as functions of elliptic integrals and can be readily evaluated. $A_0(z)$, $B_0(z)$, $C_0(z)$ and $D_0(z)$ are derived from the solution to a half-space on which a uniform pressure is applied over the area of a circle with radius a (Sneddon, 1951). A subset of these kernel solutions has been presented by Selvadurai and Rajapakse (1985).

From interface conditions (6) and eqns (7) and (8), a set of four coupled integral equations for the four functions can be derived. Alternatively, if the cracked fiber were perfectly bonded to the matrix, then the condition would be continuity of traction and displacement (6a), and again four coupled integral equations can be derived. Use will be made use of this when the method is tested on problems with a perfectly bonded interface.

These integral equations were solved numerically by a standard discretization procedure. For convenience, a change of variables

$$\zeta = \frac{1}{1+z} \tag{9}$$

is employed to transform the domain of the interface $0 < z < \infty$ to $0 < \zeta < 1$. The domain $0 < \zeta < 1$ is then divided into N equally sized intervals, and the interfacial stresses and displacement gradients σ_{rr}^{F}, σ_{rz}^{F}, $u_{r,z}^{F}$, $u_{z,z}^{F}$ and σ_{rr}^{M}, σ_{rz}^{M}, $u_{r,z}^{M}$, $u_{z,z}^{M}$ are evaluated in the mid-points of these intervals. For this evaluation the functions $p_1(z)$, $p_2(z)$, $p_3(z)$ and $p_4(z)$ are approximated as piece-wise linear functions with two exceptions. To capture the behavior of the stress field as $z \to \infty$ properly, the functions in the last interval ($z_{N-1} < z < \infty$) are approximated by a constant divided by z^{λ}. For cases in which the interface is perfectly bonded, the stress field is singular in that $\sigma \sim \rho^{-\lambda}$ as the crack tip is approached; the order of the singularity, λ, is real and depends on the relative moduli (Hein and Erdogan, 1971). Therefore in the first, say, M intervals, the functions are approximated by a linear function divided by z^{λ} to account for the singular behavior close to the crack tip. The validity of this representation is justified in Schwietert and Steif (1991). All results presented are based on $N = 40$; for singular problems, $M = 4$.

Clearly, the accuracy of this method is dependent on the discretization and on the interpolation functions that are chosen. Here, the major goal is to solve the broken fiber problem with a *frictional* interface; in previous studies of similar problems (Dollar and Steif, 1988, 1989; Steif and Dollar, 1988) piece-wise linear interpolation functions had been found to give more accurate results than, for example, the often-used Chebyshev polynomials (Erdogan *et al.*, 1973). For the purpose of testing its accuracy, this method will also be applied to some problems in which the interface is perfectly bonded; for those cases the choice of piece-wise linear interpolation functions is possibly not optimal.

4. RESULTS AND DISCUSSION

In Schwietert and Steif (1991) we applied this integral equation method to several two-dimensional test problems. Here we apply the method to two test problems, now three-dimensional problems, having the same geometry and loading as the main problem studied in this paper (Fig. 1), but having different interface conditions and elastic properties. For the first test problem, the interface is perfectly bonded and the elastic properties of the fiber and the matrix are identical. This is equivalent to the problem of a penny-shaped crack in a homogeneous material, which was solved by Sneddon (1951). For the second test problem the interface is perfectly bonded, but now the elastic properties of the matrix and the fiber are not identical. This problem was solved by Ford (1973).

In the first test problem the integral equations are set up according to eqns (6a). Now the stress field is singular, with the order of the singularity, λ, equal to 1/2. Three specific results of our calculations were compared with Sneddon's penny-crack solution: the stresses σ_{rr} and σ_{rz} along the interface, and the stress σ_{zz} on the plane $z = 0$. The error in the stresses σ_{rr} and σ_{rz} was found to be less than 0.5% over the entire range, except in the interval closest to the crack, where the error is approximately 5%. The error in σ_{zz} at the plane $z = 0$ was found to decrease with increasing r; it appears to be less than 1% for points further than $0.05a$ from the perimeter of the crack ($r > 1.05a$) and less than 0.5% for points further than $0.1a$ from the perimeter of the crack. Close to the crack the error increases significantly and is, for example, about 10% for a point at a distance of $0.001a$ from the perimeter.

In the second test problem, the integral equations were again set up according to (6a). The stress field is again singular and the order of the singularity, λ, which can be calculated from the results of the study by Hein and Erdogan (1971), is real and in the interval $0 < \lambda < 1$. For this problem the axial fiber stress, averaged over the fiber cross-section, Σ, was calculated for different combinations of material parameters G_1, ν_1, G_2, ν_2 and compared with the results of Ford (1973). This average axial fiber stress at $z = z_1$ is found by integrating the interfacial shear stress σ_{rz} from $z = 0$ to z_1:

$$\Sigma(z_1) = -\frac{2}{a}\int_0^{z_1} \sigma_{rz}\,\mathrm{d}z - p. \tag{10}$$

Comparing Σ is, therefore, tantamount to comparing σ_{rz} at the interface. Note that the average axial fiber stress is equal to $-p$ at $z = 0$ and approaches 0 as $z \to \infty$. The results were found to correspond very well with the results of Ford (within 2%), provided a correction was introduced to compensate for the error in σ_{rz} in the first interval. In this comparison, the ratio of elasticity moduli G_1/G_2 was varied from 1 to 10. The largest correction for σ_{rz} in the first interval was about 10% for the case $G_1/G_2 = 10$.

From the results of these test problems, and of the test problems presented in Schwietert and Steif (1991), one can conclude that the method proposed here can give accurate results for the main problem studied in this paper. We will focus this study on five cases, with different ratios of Young's moduli E_1/E_2. The first case corresponds to a homogeneous material, $E_1/E_2 = 1$. For the second case, we have chosen the parameters of a Nicalon-reinforced lithium–alumino-silicate glass ceramic (Prewo, 1986), which has a modulus ratio $E_1/E_2 = 2.38$. For the third case, we have chosen the parameters of Silicon carbide monofilament-reinforced borosilicate glass ceramic, which has a modulus ratio $E_1/E_2 = 6.75$ (Prewo, 1982; Prewo *et al.*, 1986). In the fourth and fifth case the modulus ratios were chosen to be the reciprocals of cases 2 and 3, with the matrix (the uncracked constituent) being stiffer than the fiber (the cracked constituent); hence $E_1/E_2 = 0.42$ and $E_1/E_2 = 0.15$, respectively. (The problem then represents a circular matrix crack which impinges on surrounding fibers.) For convenience, we have fixed $\nu_1 = \nu_2 = 0.3$ for all these cases (which makes $E_1/E_2 = G_1/G_2$), and we have chosen the Coulomb friction coefficient μ to be 0.3.

We anticipate the solution to involve slip over some portion of the interface. In particular, we expect the fiber to slip with respect to the matrix over the region $0 < |z| < L_s$. In this work, we will limit ourselves to cases which have slip, but no opening over the interface. A sufficient condition to ensure no opening is that the stress normal to the interface, σ_{rr}, is compressive over the entire interface; for the cases studied this has to be verified *a posteriori*. For this problem the integral equations are set up according to the relations (6a) and (6b). Since the problem now does not contain a singularity, the functions in the intervals close to the crack tip are also approximated as piece-wise linear.

A difficulty that arises in solving the equations is that the slip length L_s is dependent on p, μ and σ_0. For numerical convenience we fixed μ and L_s/a, and then solved the equations assuming different values of p/σ_0. The correct value of p/σ_0 corresponds to interfacial stresses and displacement gradients at the end of the slip zone satisfying both (6a) and (6b) (a smooth transition from slip to stick). Thus solved, the solutions for σ_{rr} and σ_{rz} along the interface approach zero at the crack tip, as one would expect from the two-dimensional, asymptotic stress field (Dollar and Steif, 1989; Schwietert and Steif, 1989). This suggests that, unlike the solution for the perfectly bonded problems, the error in the solution at the crack tip is small. These calculations were repeated for the five cases mentioned above; as expected, the slip length increases with increasing p/σ_0. We also carried calculations for the set of parameters $E_1/E_2 = 5$, $\nu_1 = \nu_2 = 0.25$ and $\mu = 0.5$. This case was considered by Aksel *et al.* (1991), who calculated the slip length for this using a finite element method. The results agree to within 10%.

In studying a broken weakly-bonded fiber, our focus is mainly on three particular results: the load transfer from the fiber to the matrix; the opening of the crack tip which is a consequence of the interfacial slippage; and the stress concentration near the broken fiber. One question of interest is whether the load transfer and the crack-tip opening can be estimated by approximate analyses which are ubiquitous in the composites literature [see, for example, Kelly and Davies (1965) and Marshall and Evans (1985)]. These approximate analyses assume that the shear stress at the interface is constant, say τ_0. [Note that extensions of the shear-lag method to account for variations in normal stress which can alter the friction stress have been proposed (e.g. Takaku and Arridge, 1973; Morton and Groves, 1976; Steif, 1984; Shetty, 1988). However, we compare our results only with constant

interfacial shear stress analyses since these seem to be standard in micro-mechanics models of ceramic–matrix composites.] Then, by equilibrium arguments, the average stress in a broken fiber, Σ_{app}, must be linear with distance from the break according to

$$\Sigma_{app}(z_1) = \frac{2}{a}\tau_0 z_1 - p \quad (0 < z_1 < L) \tag{11}$$

where the transfer length L/a is given by $p/2\tau_0$. Note that this approximate analysis gives a constant load transfer rate, and that all of the load is transferred over the length L.

Through the use of a concentric cylinder analysis, one can similarly estimate the slippage which causes crack-tip opening. With the linear load transfer, one can find the strains in the fiber and the matrix and then integrate over the slip length (transfer length) to obtain the jump in displacement which is the crack-tip opening. This procedure, which is better known in the case of estimating the matrix–crack opening (Marshall and Evans, 1985), leads to the following result:

$$w = \frac{p^2 a}{4\tau_0 E_1}. \tag{12}$$

The infinite-domain problem demands a great deal of any approximate analysis and more sophisticated approximate methods might conceivably be employed to estimate the opening. The point here, however, is merely to indicate the degree to which the simplest-minded approach can give reasonable answers.

Two aspects of the load transfer are of interest: the rate at which the load transfers over the slip zone and the fraction of the total load that is transferred over the slip zone. Figure 5 shows the average axial fiber stress versus z/a for case 2 and case 5, for a slip length of $L_s = 2.333a$. The applied pressure p is about $2.33\sigma_0$ in both cases. Figure 5 also shows the average axial fiber stress calculated with (11), assuming τ_0 is equal to $\mu\sigma_0$ (dashed curve). This result indicates that over the slip zone the rate of load transfer is almost constant; however, the rate is higher than if a constant shear stress $\mu\sigma_0$ is assumed and much higher if the fiber is more compliant than the matrix. This may be understood by considering the discussion of the results of other frictional interface problems (Dollar and

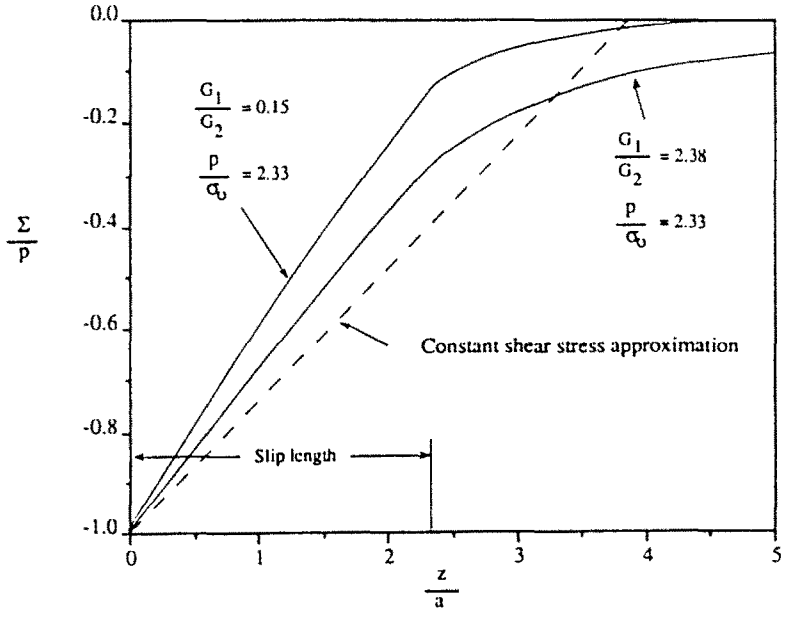

Fig. 5. Average axial fiber stress near the crack tip ($\mu = 0.3$).

Steif, 1988, 1989). There it was found that the shear stress at the interface, given by the Coulomb friction law, is itself composed of two parts: $\mu\sigma_0$ (associated with the residual stress) and the remainder, which is associated with the loading. Except for the immediate vicinity of the crack tip, the effect of pressuring open the crack is for the fiber to expand, adding to the compression at the interface. Thus, the stiffer the fiber, the less will be the expansion and, therefore, the less will be the additional interfacial shear stress. Clearly, a constant shear stress approximation can reasonably describe the load transfer from fiber to matrix over the slip zone; however, estimating that constant shear stress by $\mu\sigma_0$ becomes increasingly less accurate with decreasing G_1/G_2.

Figure 6 shows the average axial fiber stress at the end of the slip zone, Σ_e, versus the dimensionless loading parameter p/σ_0. If Σ_e were equal to 0, then all of the load would have been transmitted over the slip zone, which is the prediction of the constant shear stress approximation. Since Σ_e is, in general, less than zero, some of the load is then transferred across the nonslipping portion of the interface. Notice that more load is transmitted over the slip zone (Σ_e/p gets closer to 0) as the load p/σ_0 is increased and as the modulus ratio G_1/G_2 decreases. Coupled with the above results for the load transfer rate, it can be concluded that estimating the load transfer with a constant shear stress approximation will be more accurate with increasing p/σ_0 and with decreasing G_1/G_2, though the transfer rate must be modified more and more as G_1/G_2 decreases.

Similar calculations were performed for μ equal to 0.2 and 0.1. Again it was found that the rate of load transfer over the slip zone is almost constant; however, an approximation of this rate based on a constant shear stress $\mu\sigma_0$ becomes increasingly accurate with decreasing μ. This is consistent with the conclusions of an earlier study involving a frictional interface (Dollar and Steif, 1988). Furthermore, it was found that, for a given slip length, the average axial fiber stress at the end of the slip zone, Σ_e, is virtually independent of μ.

For the five cases considered, we also computed the crack-tip opening, w, which is defined as

$$w = \lim_{r \to a} u_z(a, 0). \tag{13}$$

Note that the crack-tip opening w is nonzero due to frictional slip at the interface. Figure 7 shows the normalized opening w/a versus the dimensionless loading parameter p/σ_0. The opening increases with increasing p/σ_0, as one would expect, and with increasing G_1/G_2. Clearly a more compliant matrix allows for more displacement of the fiber. Figure 7 also shows the opening calculated with eqn (12), assuming τ_0 is equal to $\mu\sigma_0$ (dashed curve).

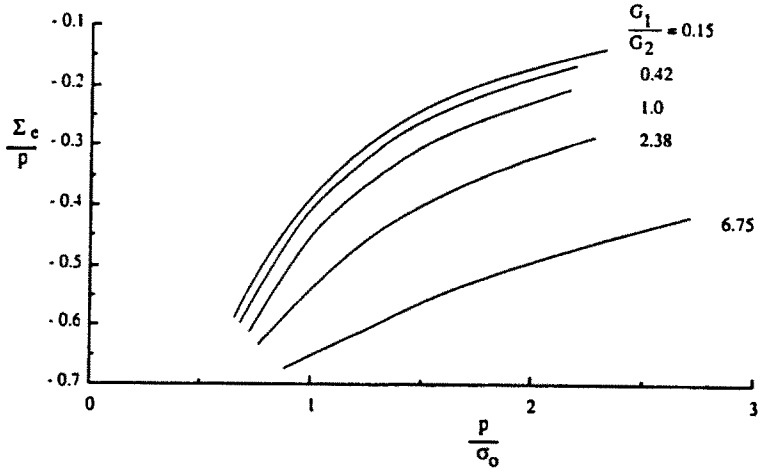

Fig. 6. Average axial fiber stress at the end of the slip zone as a function of applied pressure ($\mu = 0.3$).

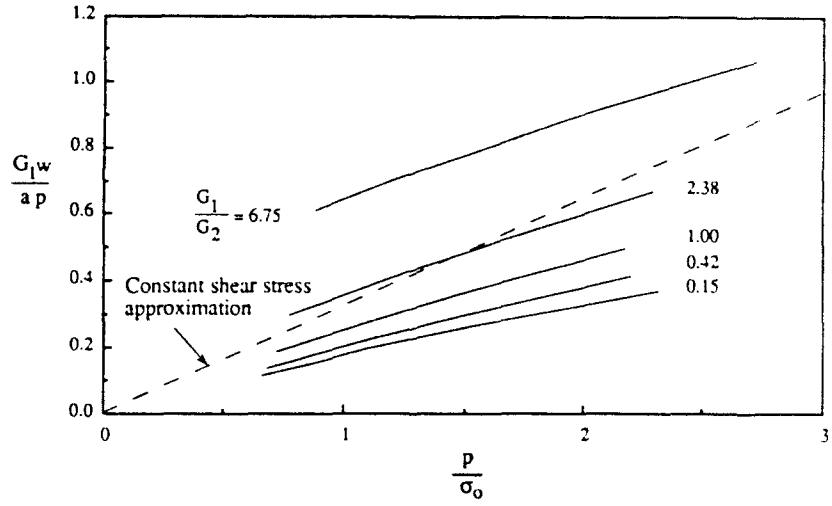

Fig. 7. Normalized opening of the crack tip as a function of applied pressure ($\mu = 0.3$).

Comparison of this approximate result with, say, the homogeneous case indicates that a simple-minded, concentric cylinder model with a constant shear stress at the interface overestimates the opening, especially for large p/σ_0.

Finally, we will consider the results for the tensile stress at the plane $z = 0$. Figure 8 shows the normalized tensile stress σ_{zz}/p in this plane versus r/a for case 1, the homogeneous case. Results are presented for five different loading levels p/σ_0, and these are compared with the normalized tensile stress σ_{zz}/p found in the case of a perfectly bonded interface. In contrast to the perfectly bonded interface problem, the tensile stress reaches a finite value at the perimeter of the crack for the frictional interface problem. However, as the zone of slip decreases, with increasing μ or with decreasing p/σ_0, the stress field approaches the

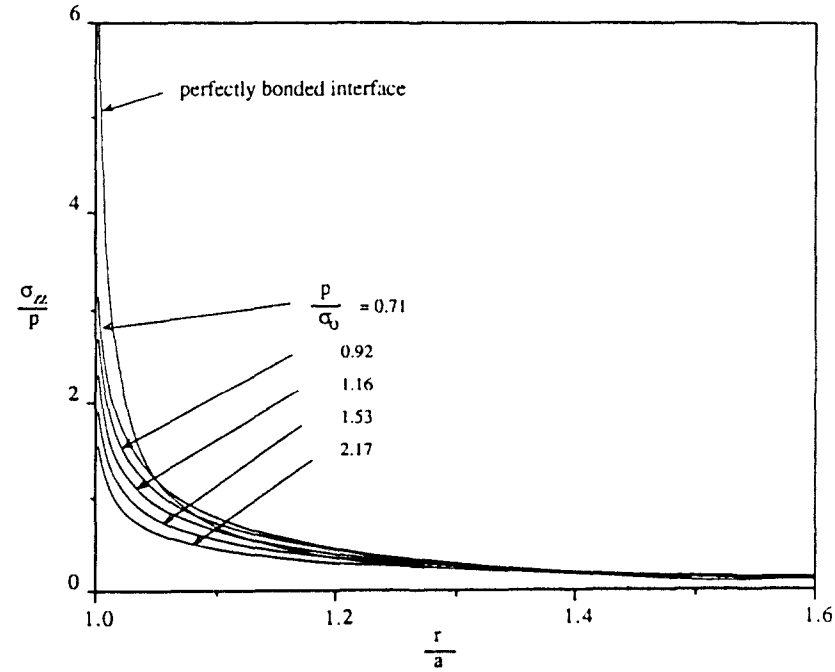

Fig. 8. Tensile stress ahead of the crack tip ($\mu = 0.3$, $G_1/G_2 = 1.0$).

perfectly bonded stress field. As the load increases, the interface "blunts" the crack more and more in the sense that the stress concentration diminishes; the magnitude of this stress concentration is found to be about the same as in the two-dimensional idealization of this problem, which was studied in Schwietert and Steif (1991). Furthermore, it was found that this stress concentration, for given p/σ_0, is rather insensitive to the relative modulus E_1/E_2.

We also considered the distance over which the tensile stress decreases. This could give some insight into the influence of a broken fiber on the stress in neighboring fibers. Consider, therefore, a composite with fiber volume fraction 0.5. If the fibers are ordered in a hexagonal array, then the distance between the perimeters of two fibers would be about $0.7a$. Figure 8 shows that the tensile stress decreases quite rapidly away from the crack and that the decrease is roughly the same for the frictional interface problem as for the perfectly bonded interface problem. Our calculations indicate that, for the example of p/σ_0 equal to 1.16, σ_{zz}/p is approximately equal to 0.1 at $r = 1.7a$. Furthermore, this enhancement in stress is only over a small region around the plane $z = 0$; for increasing z (at $r = 1.7a$), σ_{zz}/p remains roughly equal to 0.1 up to z/a equal to 0.5 and decreases quite rapidly thereafter. This suggests that the influence of fiber breaks on neighboring fibers may be relatively small.

5. SUMMARY

The problem of a single broken fiber which is connected by friction to an infinite matrix has been studied. Using a new integral equation method, the solution to this problem has been reduced to four simultaneous integral equations which have solved numerically. Particular results of interest have been the rate at which load is transferred between the fiber and the matrix, the opening of the crack due to interfacial slippage, and the stress enhancement near the fiber break. Consistent with simple analyses, the load transfer near the break has been found to be nearly linear. However, the slope is influenced by the relative moduli, and by the particular combination of residual interfacial pressure and friction coefficient. Also, the proportion of load that is transferred over the slip zone can be small, although it increases with the level of the applied stress. The opening of the crack is vaguely similar to the predictions of simplified analyses, though the quantitative dependence on parameters is more complicated; not surprisingly, there is a substantial dependence on relative modulus. As was found in previous studies of cracks impinging on frictional interfaces, the interface causes the tensile stress at the tip to be finite; the stress concentration diminishes with the applied load. Furthermore, the decrease of stress with distance ahead of the break is sufficiently rapid that any influence of one fiber break on a neighboring fiber seems unlikely as long as the matrix stays intact.

Acknowledgements—The authors are grateful to the Department of Energy for the support of HRS under grant DE-FG02-89ER45404 and to the Air Force Office of Scientific Research, for the support of PSS under grant AFOSR 890548. In addition, the support by the Department of Mechanical Engineering, Carnegie Mellon University is gratefully acknowledged.

REFERENCES

Aksel, B., Lagoudas, D. C. and Hui, C. Y. (1991). Effects of a frictional interface on debonding in a fiber-reinforced composite. *Int. J. Solids Structures* **27**, 833–847.

Dollar, A. and Steif, P. S. (1988). Load transfer in composites with a coulomb friction interface. *Int. J. Solids Structures* **24**, 789–803.

Dollar, A. and Steif, P. S. (1989). A tension crack impinging upon frictional interfaces. *J. Appl. Mech.* **56**, 291–298.

Dundurs, J. (1967). Effect of elastic constants on stress in a composite under plane deformation. *J. Comp. Mater.* **1**, 310–322.

Eason, G., Noble, B. and Sneddon, I. N. (1955). On certain integrals of Lipschitz-Hankel type involving products of Bessel functions. *Philos. Trans. R. Soc. London A* **247**, 529–551.

Erdogan, F., Gupta, G. D. and Cook, T. S. (1973). Numerical solutions of singular integral equations. In *Mechanics of Fracture* (Edited by G. C. Sih), Chapter 7. Noordhoff, Leiden.

Ford, E. F. (1973). Stress analysis of a broken fiber embedded in an elastic medium. Report No. 1, Division of Engineering and Applied Physics, Harvard University.

Hein, V. L. and Erdogan, F. (1971). Stress singularities in a two-material wedge. *Int. J. Fract. Mech.* **7**, 317–330.

Kelly, A. and Davies, G. J. (1965). The principles of the fibre reinforcement of metals. *Met. Rev.* **10**, 1–77.

Marshall, D. B. and Evans, A. G. (1985). Failure mechanisms in ceramic-fibre ceramic-matrix composites. *J. Am. Ceram. Soc.* **68**, 225–231.
Morton, J. and Groves, G. W. (1976). The effect of metal wires on the fracture of a brittle matrix composite. *J. Mater. Sci.* **11**, 617–622.
Muki, R. and Sternberg, E. (1971). Load-absorption by a discontinuous filament in a fiber-reinforced composite. *ZAMP* **22**, 809–824.
Phillips, D. C. (1974). Interfacial bonding and the toughness of carbon fibre reinforced glass and glass-ceramics. *J. Mater. Sci.* **9**, 1847–1854.
Prewo, K. M. (1982). A compliant, high failure strain, fibre-reinforced glass–matrix composite. *J. Mater. Sci.* **17**, 3549–3563.
Prewo, K. M. (1986). Tension and flexural strength of silicon carbide fibre-reinforced glass ceramics. *J. Mater. Sci.* **21**, 3590–3600.
Prewo, K. M. and Brennan, J. J. (1980). High-strength silicon carbide fibre-reinforced glass–matrix composites. *J. Mater. Sci.* **15**, 463–468.
Prewo, K. M., Brennan, J. J. and Layden, G. K. (1986). Fiber reinforced glasses and glass-ceramics for high performance applications. *Am. Cer. Soc. Bull.* **65**, 305–314.
Schwietert, H. R. and Steif, P. S. (1991). An interface integral equation method applied to a crack impinging upon a bimaterial, frictional interface. *Int. J. Fract.* (to appear).
Selvadurai, A. P. S. and Rajapakse, R. K. N. D. (1985). On the load transfer from a rigid cylindrical inclusion into an elastic half space. *Int. J. Solids Structures* **21**, 1213–1229.
Shetty, D. K. (1988). Shear-lag analysis of fiber pushout (indentation) tests for estimating interfacial friction stress in ceramic-matrix composites. *J. Am. Cer. Soc.* **71**, C-107–C-109.
Sneddon, I. N. (1951). *Fourier Transforms*. McGraw-Hill, New York.
Steif, P. S. (1984). Stiffness reduction due to fiber breakage. *J. Comp. Mater.* **18**, 153–172.
Steif, P. S. and Dollar, A. (1988). Longitudinal shearing of a weakly bonded fiber composite. *J. Appl. Mech.* **55**, 618–623.
Takaku, A. and Arridge, R. G. C. (1973). The effect of interfacial radial and shear stresses on fibre pull-out in composite materials. *J. Phys. D: Appl. Phys.* **6**, 2038–2047.
Timoshenko, S. P. and Goodier, J. N. (1970). *Theory of Elasticity*. McGraw-Hill, New York.
Wang, Y. C., Hui, C. Y., Lagoudas, D. and Papadopoulos, J. (1989). Small-scale crack blunting at a bimaterial interface with Coulomb friction. *Int. J. Fract.* (to appear).
Zak, A. R. (1964). Stresses in the vicinity of boundary discontinuities in bodies of revolution. *J. Appl. Mech.* **31**, 150–152.

APPENDIX

Herein, we give expressions for the stresses and the displacement gradients associated with concentrated unit ring forces. The kernels in the integral eqns (7) and (8) are obtained by setting $r = r' = a$.

Concentrated unit ring force in the radial direction at (r', z') *in an infinite medium*

$$\sigma_{rz}(r,z)|_1 = \int_0^\infty \frac{2r'}{8(1-\nu)}\{\operatorname{sgn}(z-z')\,e^{-\xi|z-z'|}\xi[-2+2\nu] + e^{-\xi|z-z'|}\xi^2[z-z']\}J_1(\xi r')J_1(\xi r)\,d\xi$$

$$\sigma_{rr}(r,z)|_1 = \int_0^\infty \frac{2r'}{8(1-\nu)}\{e^{-\xi|z-z'|}\xi[3-2\nu] - e^{-\xi|z-z'|}\xi^2[|z-z'|]\}J_1(\xi r')J_0(\xi r)\,d\xi$$

$$-\frac{1}{r}\int_0^\infty \frac{2r'}{8(1-\nu)}\{e^{-\xi|z-z'|}[\lambda_1] - e^{-\xi|z-z'|}\xi[|z-z'|]\}J_1(\xi r')J_1(\xi r)\,d\xi$$

$$u_{rz}(r,z)|_1 = \int_0^\infty \frac{r'}{8G(1-\nu)}\{\operatorname{sgn}(z-z')\,e^{-\xi|z-z'|}\xi[-\lambda_1+1] + e^{-\xi|z-z'|}\xi^2[z-z']\}J_1(\xi r')J_1(\xi r)\,d\xi$$

$$u_{rr}(r,z)|_1 = \int_0^\infty \frac{r'}{8G(1-\nu)}\{-e^{-\xi|z-z'|}\xi + e^{-\xi|z-z'|}\xi^2[|z-z'|]\}J_1(\xi r')J_0(\xi r)\,d\xi.$$

Concentrated unit ring force in the axial direction at (r', z') *in an infinite medium*

$$\sigma_{rz}(r,z)|_4 = \int_0^\infty \frac{2r'}{8(1-\nu)}\{-e^{-\xi|z-z'|}\xi - e^{-\xi|z-z'|}\xi^2[|z-z'|] + 2\nu\,e^{-\xi|z-z'|}\xi\}J_0(\xi r')J_1(\xi r)\,d\xi$$

$$\sigma_{rr}(r,z)|_4 = \int_0^\infty \frac{2r'}{8(1-\nu)}\{[\operatorname{sgn}(z-z')\,e^{-\xi|z-z'|}\xi + e^{-\xi|z-z'|}\xi^2[z-z']] + (1+2\nu)[-\operatorname{sgn}(z-z')\,e^{-\xi|z-z'|}\xi]\}J_0(\xi r')J_0(\xi r)\,d\xi$$

$$-\frac{1}{r}\int_0^\infty \frac{2r'}{8(1-\nu)}\{e^{-\xi|z-z'|}\xi[z-z']\}J_0(\xi r')J_1(\xi r)\,d\xi$$

$$u_{r,z}(r,z)|_4 = \int_0^\infty \frac{r'}{8G(1-\nu)}\{e^{-\xi(z+z')}\xi - e^{-\xi|z-z'|}\xi^2[|z-z'|]\}J_0(\xi r')J_1(\xi r)\,d\xi$$

$$u_{z,z}(r,z)|_4 = \int_0^\infty \frac{r'}{8G(1-\nu)}\{\mathrm{sgn}\,(z-z')\,e^{-\xi(z+z')}\xi[-\lambda_1+1] - e^{-\xi|z-z'|}\xi^2[z-z']\}J_0(\xi r')J_0(\xi r)\,d\xi.$$

Concentrated unit ring force in the radial direction at (r′, z′) *in a semi-infinite medium*

$$\sigma_{r,z}(r,z)|_1 = \int_0^\infty \frac{2r'}{8(1-\nu)}\{[e^{-\xi(z+z')}\xi[\lambda_1-\lambda_2] + e^{-\xi|z-z'|}\xi^2[\lambda_1(z'+z)-2z'] + e^{-\xi|z-z'|}\xi^3[-2z'z]]$$

$$+\nu[e^{-\xi(z+z')}\xi[-2\lambda_1] + e^{-\xi|z-z'|}\xi^2[4z']]\}J_1(\xi r')J_1(\xi r)\,d\xi + \sigma_{r,z}(r,z)|_3$$

$$\sigma_{\theta\theta}(r,z)|_1 = \int_0^\infty \frac{2r'}{8(1-\nu)}\{[e^{-\xi(z+z')}\xi[\lambda_2-\lambda_1] + e^{-\xi|z-z'|}\xi^2[-\lambda_1(z+z')+2z'] + e^{-\xi|z-z'|}\xi^3[2z'z]]$$

$$+(1+2\nu)[e^{-\xi(z+z')}\xi[\lambda_1] + e^{-\xi|z-z'|}\xi^2[-2z']]\}J_1(\xi r')J_0(\xi r)\,d\xi - \frac{1}{r}\int_0^\infty \frac{2r'}{8(1-\nu)}[e^{-\xi(z+z')}[\lambda_2]$$

$$+e^{-\xi(z+z')}\xi[-\lambda_1(z+z')] + e^{-\xi|z-z'|}\xi^2[2z'z]]J_1(\xi r')J_1(\xi r)\,d\xi + \sigma_{\theta\theta}(r,z)|_3$$

$$u_{r,z}(r,z)|_1 = \int_0^\infty \frac{r'}{8G(1-\nu)}[e^{-\xi(z+z')}\xi[-\lambda_1-\lambda_2] + e^{-\xi|z-z'|}\xi^2[\lambda_1(z+z')+2z']$$

$$+e^{-\xi|z-z'|}\xi^3[-2z'z]]J_1(\xi r')J_1(\xi r)\,d\xi + u_{r,z}(r,z)|_3$$

$$u_{z,z}(r,z)|_1 = \int_0^\infty \frac{r'}{8G(1-\nu)}[e^{-\xi(z+z')}\xi[-\lambda_1+\lambda_3] + e^{-\xi|z-z'|}\xi^2[\lambda_1(z-z')+2z']$$

$$+e^{-\xi|z-z'|}\xi^3[-2z'z]]J_1(\xi r')J_0(\xi r)\,d\xi + u_{z,z}(r,z)|_3.$$

Concentrated unit ring force in the axial direction at (r′, z′) *in a semi-infinite medium*

$$\sigma_{r,z}(r,z)|_2 = \int_0^\infty \frac{2r'}{8(1-\nu)}\{[e^{-\xi(z+z')}\xi[-\lambda_1+\lambda_3] + e^{-\xi|z-z'|}\xi^2[\lambda_1(z'-z)-2z'] + e^{-\xi|z-z'|}\xi^3[-2z'z]]$$

$$+\nu[e^{-\xi(z+z')}\xi[2\lambda_1] + e^{-\xi|z-z'|}\xi^2[4z']]\}J_0(\xi r')J_1(\xi r)\,d\xi + \sigma_{r,z}(r,z)|_4$$

$$\sigma_{\theta\theta}(r,z)|_2 = \int_0^\infty \frac{2r'}{8(1-\nu)}\{[e^{-\xi(z+z')}\xi[\lambda_1-\lambda_3] + e^{-\xi|z-z'|}\xi^2[\lambda_1(z-z')+2z'] + e^{-\xi|z-z'|}\xi^3[2z'z]]$$

$$+(1+2\nu)[e^{-\xi(z+z')}\xi[-\lambda_1] + e^{-\xi|z-z'|}\xi^2[-2z']]\}J_0(\xi r')J_0(\xi r)\,d\xi - \frac{1}{r}\int_0^\infty \frac{2r'}{8(1-\nu)}[e^{-\xi(z+z')}[-\lambda_3]$$

$$+e^{-\xi(z+z')}\xi[\lambda_1(z-z')] + e^{-\xi|z-z'|}\xi^2[2z'z]]J_0(\xi r')J_1(\xi r)\,d\xi + \sigma_{\theta\theta}(r,z)|_4$$

$$u_{r,z}(r,z)|_2 = \int_0^\infty \frac{r'}{8G(1-\nu)}[e^{-\xi(z+z')}\xi[\lambda_1+\lambda_3] - e^{-\xi|z-z'|}\xi^2[\lambda_1(z-z')-2z']$$

$$+e^{-\xi|z-z'|}\xi^3[-2z'z]]J_0(\xi r')J_1(\xi r)\,d\xi + u_{r,z}(r,z)|_4$$

$$u_{z,z}(r,z)|_2 = \int_0^\infty \frac{r'}{8G(1-\nu)}[e^{-\xi(z+z')}\xi[\lambda_1-\lambda_2] + e^{-\xi|z-z'|}\xi^2[-\lambda_1(z+z')+2z']$$

$$+e^{-\xi|z-z'|}\xi^3[-2z'z]]J_0(\xi r')J_0(\xi r)\,d\xi + u_{z,z}(r,z)|_4$$

where:

$$\lambda_1 = (3-4\nu);\quad \lambda_2 = (8\nu^2-12\nu+5);\quad \lambda_3 = 4(1-\nu)(1-2\nu).$$